

Ozone Exposure Response for U.S. Soybean Cultivars: Linear Reductions in Photosynthetic Potential, Biomass, and Yield^{1[W][OA]}

Amy M. Betzelberger, Craig R. Yendrek, Jindong Sun², Courtney P. Leisner, Randall L. Nelson, Donald R. Ort, and Elizabeth A. Ainsworth*

Department of Plant Biology (A.M.B., C.P.L., D.R.O., E.A.A.), Institute for Genomic Biology (C.R.Y., J.S., D.R.O., E.A.A.), and Department of Crop Sciences (R.L.N.), University of Illinois, Urbana-Champaign, Illinois 61801; and Soybean/Maize Germplasm, Pathology, and Genetics Research Unit (R.L.N., E.A.A.) and Global Change and Photosynthesis Research Unit (C.R.Y., D.R.O., E.A.A.), United States Department of Agriculture Agricultural Research Service, Urbana, Illinois 61801

Current background ozone (O₃) concentrations over the northern hemisphere's midlatitudes are high enough to damage crops and are projected to increase. Soybean (*Glycine max*) is particularly sensitive to O₃; therefore, establishing an O₃ exposure threshold for damage is critical to understanding the current and future impact of this pollutant. This study aims to determine the exposure response of soybean to elevated tropospheric O₃ by measuring the agronomic, biochemical, and physiological responses of seven soybean genotypes to nine O₃ concentrations (38–120 nL L⁻¹) within a fully open-air agricultural field location across 2 years. All genotypes responded similarly, with season-long exposure to O₃ causing a linear increase in antioxidant capacity while reducing leaf area, light absorption, specific leaf mass, primary metabolites, seed yield, and harvest index. Across two seasons with different temperature and rainfall patterns, there was a robust linear yield decrease of 37 to 39 kg ha⁻¹ per nL L⁻¹ cumulative O₃ exposure over 40 nL L⁻¹. The existence of immediate effects of O₃ on photosynthesis, stomatal conductance, and photosynthetic transcript abundance before and after the initiation and termination of O₃ fumigation were concurrently assessed, and there was no evidence to support an instantaneous photosynthetic response. The ability of the soybean canopy to intercept radiation, the efficiency of photosynthesis, and the harvest index were all negatively impacted by O₃, suggesting that there are multiple targets for improving soybean responses to this damaging air pollutant.

Modern-day annual average background tropospheric ozone (O₃) concentrations [O₃] over the midlatitudes of the northern hemisphere are more than double the levels measured over a century ago (Vingarzan, 2004). Current [O₃] are high enough to cause damage to crops, and among the four major global food crops, soybean (*Glycine max*) is particularly sensitive to O₃ (Emberson et al., 2009), with models indicating reductions of global soybean yields by 8.5% to 14% in 2000 (Avnery et al., 2011a). Background [O₃] are increasing by an average of 0.3 nL L⁻¹ per year as a

result of increased human activity (Wilkinson et al., 2012). While the exact future [O₃] will depend upon regional and global emissions, enactment and adherence to air-quality legislation, and climate change (Stevenson et al., 2006), the potential increases in background [O₃] are predicted to induce soybean yield losses of 9% to 19% by 2030 (Avnery et al., 2011b).

O₃ decreases crop yields by a number of different mechanisms (Fiscus et al., 2005). Upon entry through the stomata, O₃ breaks down into other reactive oxygen species, which can overwhelm the antioxidant-quenching capacity of the apoplast and, at acute concentrations, initiate a signal transduction pathway resulting in cell death (Overmyer et al., 2003; Kangasjärvi et al., 2005). The effect of a burst of acute O₃, typically defined to be short bursts of O₃ over 100 nL L⁻¹ (Chen et al., 2009), on gas exchange has been characterized by a rapid but transient decrease in stomatal conductance (g_s ; Kollist et al., 2007; Vahisalu et al., 2010), which coincides with a reactive oxygen species burst in the guard cells (Vahisalu et al., 2010). This transient decrease in g_s is not thought to be associated with a decrease in photosynthesis in the mesophyll cells, as full recovery of g_s is established within 30 to 40 min of the O₃ treatment (Kollist et al., 2007). Exposure of *Arabidopsis thaliana* to acute [O₃] also causes a suite of

¹ This work was supported by the U.S. Department of Agriculture Agricultural Research Service and the Agriculture and Food Research Initiative (competitive grant no. 2010-65114-20355 to E.A.A.) from the U.S. Department of Agriculture National Institute of Food and Agriculture.

² Present address: DuPont Pioneer, Johnston, IA 50131.

* Corresponding author; e-mail lisa.ainsworth@ars.usda.gov.

The author responsible for distribution of materials integral to the findings presented in this article in accordance with the policy described in the Instructions for Authors (www.plantphysiol.org) is: Elizabeth A. Ainsworth (lisa.ainsworth@ars.usda.gov).

^[W] The online version of this article contains Web-only data.

^[OA] Open Access articles can be viewed online without a subscription. www.plantphysiol.org/cgi/doi/10.1104/pp.112.205591

transcriptional changes that overlap with common oxidative stress pathways (Gadjev et al., 2006). However, chronic or long-term exposure of plants in the field to lower $[O_3]$ does not necessarily elicit the same transcriptional or metabolite response as short-term acute O_3 exposure (Gillespie et al., 2012). At lower concentrations, O_3 may not cause visible necrotic lesions on leaves but can negatively impact photosynthetic carbon gain via effects on the Calvin cycle and light-harvesting processes (Goumenaki et al., 2010; Sarkar et al., 2010) and by accelerating senescence (Pell et al., 1997). Exposure to elevated $[O_3]$ also fundamentally alters other aspects of metabolism, including increased demand for respiratory energy and increased flux through the shikimate, phenylpropanoid, and anapleurotic pathways (Dizengremel et al., 2009, 2012). These changes in metabolism all have the potential to alter the efficiency by which plants capture light energy, convert that energy into carbon, and partition the carbon into biomass and harvestable yield. An early analysis of the effects of O_3 on soybean yield potential concluded that O_3 altered the ability of plants to utilize intercepted radiation but did not affect the ability of the canopy to intercept radiation or allocate aboveground biomass to seed yield (Leadley et al., 1990).

Establishing an O_3 threshold for damage to sensitive species has been an active area of research (Fuhrer et al., 1997), and knowledge of these levels is critical for establishing O_3 control strategies to minimize the harmful effects of this pollutant on plants (Emberson et al., 2000). The effects of different concentrations of O_3 on soybean productivity have been examined for decades, and syntheses of the studies done to date indicate that 30 to 50 $nL L^{-1} O_3$ can significantly reduce soybean yields (Heagle, 1989; Morgan et al., 2003). Recently, Mills et al. (2007) recompiled a large number of crop-response data from the extensive, multifield studies done in the United States and Europe in the 1980s. Using an accumulated exposure over a threshold of 40 $nL L^{-1}$ (AOT40), the critical level for damage to soybean (i.e. the level required to cause a 5% reduction in yield) was 4.3 ppm h over 3 months (Mills et al., 2007). This threshold is regularly exceeded over much of the soybean-growing region in the northern hemisphere. For example, 7 of the last 10 years in central Illinois have experienced growing season $[O_3]$ that exceeded this critical level for damage. However, it is known that plant responses to O_3 vary considerably with other environmental conditions, including air temperature and water availability (Heagle, 1989). It is also known that O_3 exposure does not always adequately predict O_3 flux into the leaf (Ashmore et al., 2004; Fares et al., 2010). Therefore, repeating O_3 exposure-response experiments in a single location in different years could help determine the robustness of a crop's O_3 exposure response.

This study takes a multifaceted approach to determine the exposure response of soybean to elevated tropospheric $[O_3]$ by measuring biochemical and

physiological responses and agronomic yield on the same cohort of plants, within one location, across two growing seasons, under fully open-air agricultural conditions. Seven soybean cultivars were investigated to determine the general response of maturity group II to IV lines to a range of $[O_3]$. Maturity group refers to the geographic range to which a soybean line is adapted, and group II to IV lines are best adapted to the latitude range of 37° to 42° N (Zhang et al., 2007). This study also concurrently assessed the instantaneous effects of O_3 exposure by taking diurnal measurements of photosynthesis, stomatal conductance, and measuring relative abundance of photosynthetic transcripts before and after the initiation and termination of daily O_3 fumigation over four time points across the growing season. The hypothesis that soybean productivity will have a negative linear response to increasing $[O_3]$ was tested by measuring photosynthetic carbon uptake, leaf area accumulation, and seed yield. It was also hypothesized that there would be a tradeoff between antioxidant metabolism and primary metabolism that was exacerbated at higher $[O_3]$ and that would be apparent in leaf-level metabolites. The synthesis of one set of metabolites might divert resources away from the synthesis of other sets of metabolites (Stitt et al., 2010), so we hypothesized that metabolite profiling would identify the tradeoffs between primary metabolism and defense. The third hypothesis tested was that acute $[O_3]$ initiates a rapid transcriptional response that impacts photosynthetic rates. Our results indicate that any increase in background $[O_3]$ above current concentrations (approximately 38 $nL L^{-1}$ during the day in these experiments) is sufficient to cause a linear decrease in seed yield, and the drivers of that yield loss include reduced cumulative leaf area index and light interception, decreased activity of Rubisco and subsequent carbon gain, and decreased harvest index.

RESULTS

O_3 Exposure-Response Experiment

In 2009 and 2010, seven soybean cultivars in maturity groups II to IV (Table I) were exposed to nine different concentrations of O_3 , ranging from ambient to a target concentration of 200 $nL L^{-1}$. Fumigation began shortly after emergence in both years, and plots were fumigated with air enriched with O_3 for 8 to 9 h daily, except when leaves were wet. In 2009, the O_3 fumigation targets were set 5 to 10 $nL L^{-1}$ higher than in 2010, leading to higher AOT40 values and a wider spread of treatment values at the end of the first growing season. In concert with these O_3 exposure differences, the 2009 growing season had lower and more variable light levels (average daily maximum photon flux density of photosynthetically active radiation [PPFD] of $1,739 \pm 432 \mu mol m^{-2} s^{-1}$) and lower air temperatures (average daily maximum temperature of $25.4^\circ C \pm 3.4^\circ C$) as well as more rainfall (total

Table 1. List and description of soybean cultivars used in the study

Cultivar	Year of Release	Maturity Group	Female Parent	Male Parent
Pioneer 93B15	2000	III		
Dwight	1997	II	Jack	A86-303014
HS93-4118	2000	IV	IA-2007	DSR 304
IA-3010	1998	III	J285	S29-39
LN97-15076	2003	IV	Macon	Stressland
Loda	2000	II	Jack	IA3003
Pana	1997	III	Jack	A3205

growing season precipitation of 370 mm) than the 2010 growing season (Supplemental Fig. S1; PPFD of $1,808 \pm 336 \mu\text{mol m}^{-2} \text{s}^{-1}$, $27.1^\circ\text{C} \pm 4.5^\circ\text{C}$, precipitation of 314 mm). Data were collected for seven cultivars, and all showed similar responses to the range of experimental $[\text{O}_3]$. Individual Student's *t* tests between cultivars did not reveal significant differences in the slopes of the O_3 responses for most parameters, so data for all genotypes were pooled. The figures provide the mean response of the seven genotypes \pm the 95% confidence intervals surrounding the mean.

Chronic Elevated O_3 Reduces Leaf Area, Light Absorption, and Specific Leaf Mass

Leaf area index (LAI) was monitored every week throughout the growing seasons of 2009 and 2010. Functional LAI, determined by integrating the area under the seasonal LAI curve and dividing by the length of the growing season, decreased linearly with increased $[\text{O}_3]$ (Fig. 1, top panel). The decrease in functional LAI with increasing $[\text{O}_3]$ was a consequence of both a shorter growing season (days; 2009 slope = -0.098 , $r^2 = 0.67$, $P = 0.013$; 2010 slope = -0.082 , $r^2 = 0.71$, $P = 0.009$) and a decrease in maximum LAI. Peak LAI fell from 6.5 in ambient $[\text{O}_3]$ to 4.3 in the highest $[\text{O}_3]$ in 2009 and from 6.4 to 4.7 in 2010 (data not shown). In addition to decreased LAI, leaf reflectance and transmittance as measured with an integrating sphere increased with increasing $[\text{O}_3]$, resulting in a significant decrease in leaf absorptance in 2010 (Fig. 1). The decrease in absorptance was associated with significantly decreased specific leaf mass in both years (Fig. 1) and seasonal leaf chlorophyll content in 2009 (g m^{-2} ; 2009 slope = -0.008 , $r^2 = 0.46$, $P = 0.045$; 2010 slope = -0.008 , $r^2 = 0.21$, $P = 0.211$).

Chronic, Not Instantaneous, Effects of O_3 on Photosynthesis

Midday measurements of photosynthetic rate (*A*) made four times over the course of each growing season in 2009 and 2010 showed a season average linear reduction in *A* of 0.06 to 0.21 $\mu\text{mol m}^{-2} \text{s}^{-1}$ per nL L^{-1} increase in $[\text{O}_3]$. The response during reproductive growth is shown in Figure 2, when loss of carbon gain to O_3 exposure would have the greatest

effect on seed yield. A significant linear relationship between *A* and O_3 exposure (AOT40) was apparent throughout the growing season, although the magnitude of the relationship was greater later in the season (data not shown), consistent with accelerated rates of senescence in elevated $[\text{O}_3]$ further exacerbating the effect on photosynthesis. g_s , the maximum activity of Rubisco ($V_{c,\text{max}}$), and the maximum rate of electron transport (J_{max}) also showed linear reductions during reproductive growth with increasing $[\text{O}_3]$ (Fig. 2), although the stomatal response was not always

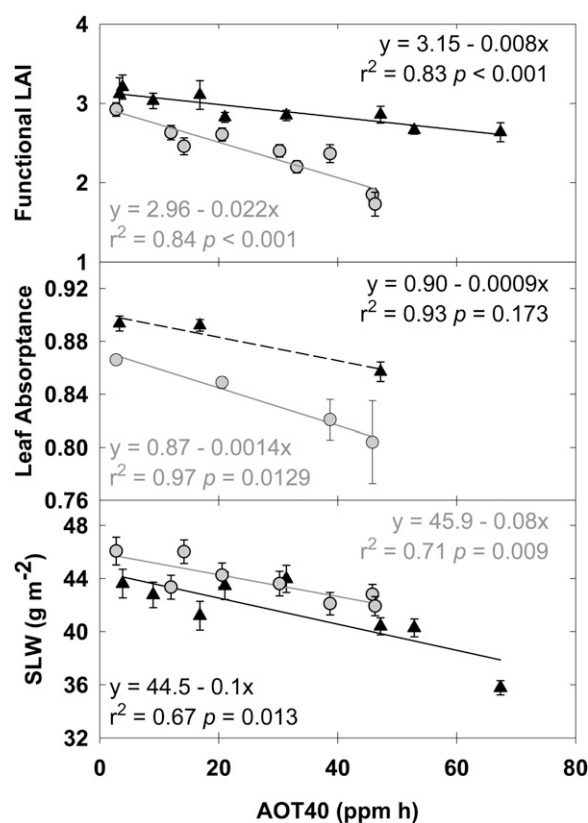


Figure 1. Linear regressions of functional LAI (top panel), leaf absorptance (middle panel), and specific leaf mass (SLW; bottom panel), which were measured throughout the growing season in 2009 (black triangles) and 2010 (gray circles). Solid lines indicate statistically significant relationships ($P < 0.05$), while dashed lines indicate nonsignificant trends. Error bars represent 95% confidence intervals.

significant (Fig. 2). Absolute values of $V_{c,max}$ and J_{max} were higher in 2010 compared with 2009, because the light intensity used to take the measurements was $2,000 \mu\text{mol m}^{-2} \text{s}^{-1}$ in 2010 and only $1,500 \mu\text{mol m}^{-2} \text{s}^{-1}$ in 2009. Still, the slopes of the responses to increasing $[\text{O}_3]$ were similar. Part of the reduction in A and g_s can be attributed to cellular damage, illustrated by lesions in the abaxial epidermis, increased wax deposition, and subsequent lower rate of chlorophyll leaching with increasing O_3 exposure (Supplemental Fig. S2).

Since several treatment plots had target $[\text{O}_3]$ high enough to be considered an acute treatment (greater than 100 nL L^{-1} ; Table II), gas exchange was monitored from approximately 10 AM to approximately 3 PM in a subset of those plots to identify metabolic changes that may occur in response to O_3 immediately following the onset and/or conclusion of fumigation. This period of the day is when photosynthesis is typically maximal and relatively invariant in field-grown plants (Bernacchi et al., 2006). If an instant response to chronic O_3 is present in these plants, a transient decrease in photosynthesis and conductance immediately following O_3 fumigation would be expected. Conversely, an increase in photosynthesis and conductance would be expected immediately following the termination of O_3 fumigation. Consistent with the midday measurements (Fig. 2), a decrease in net assimilation (2009 and 2010) and stomatal conductance (2009 only) was observed in elevated O_3 (130 nL L^{-1}) at every time sampled throughout the day (Fig. 3). However, no dynamic changes were detected in response to the onset (between 10 AM and 11:30 AM) or after the conclusion (between 2 PM and 3:30 PM) of O_3 fumigation.

A lack of an instantaneous response to high $[\text{O}_3]$ was also observed at the level of transcriptional regulation (Fig. 4). Transcript abundance of key genes involved with the light reactions of photosynthesis (*Ferredoxin thioredoxin reductase [Ftr]*, *Light-harvesting complex5a [Lhc5a]*, *Cytochrome b6f [Cyt b6f]*, and *ATP synthase [ATPase]*) as well as the Calvin cycle (*Rubisco* and *Sedoheptulose-1,7-bisphosphatase [SBPase]*) was quantified throughout the day. As all of these genes are regulated by light, the increase in abundance that was detected in ambient conditions for FTR, Rubisco, and SBPase (between 10 AM and 11:30 AM) and the decrease in abundance for LHC5A (between 10 AM and 2 PM) and SBPase (between 10 AM and 3:30 PM) was likely due to differences in the average light conditions for each sampling time (10 AM, $1,275 \mu\text{mol m}^{-2} \text{s}^{-1}$; 11:30 AM, $1,800 \mu\text{mol m}^{-2} \text{s}^{-1}$; 2 PM, $1,588 \mu\text{mol m}^{-2} \text{s}^{-1}$; 3:30 PM, $1,300 \mu\text{mol m}^{-2} \text{s}^{-1}$). Expression of each of the photosynthesis-related targets was down-regulated by 40% to 60% in $130 \text{ nL L}^{-1} [\text{O}_3]$ (Fig. 4), which was consistent with the magnitude of change for net assimilation (Fig. 3).

O_3 Decreases Metabolites Associated with Primary Metabolism and Increases Antioxidant Capacity

In concert with photosynthetic measurements, leaf tissue samples for measuring Glc, Fru, Suc, total protein, total starch, total antioxidant capacity, and phenolic content were taken at four midday time points across both growing seasons. Most relevant to seed yield is the response of these metabolites to elevated $[\text{O}_3]$ at the fourth sampling, which was during reproductive growth (September 1, 2009, and

Figure 2. Linear regressions of midday measurements of A , g_s , $V_{c,max}$, and J_{max} which were made during reproductive growth in 2009 (black triangles) and 2010 (gray circles). Cumulative AOT40 was summed from the beginning of the growing season up to the date of measurement in each year. Solid lines indicate statistically significant relationships, while dashed lines indicate trends. Error bars represent 95% confidence intervals.

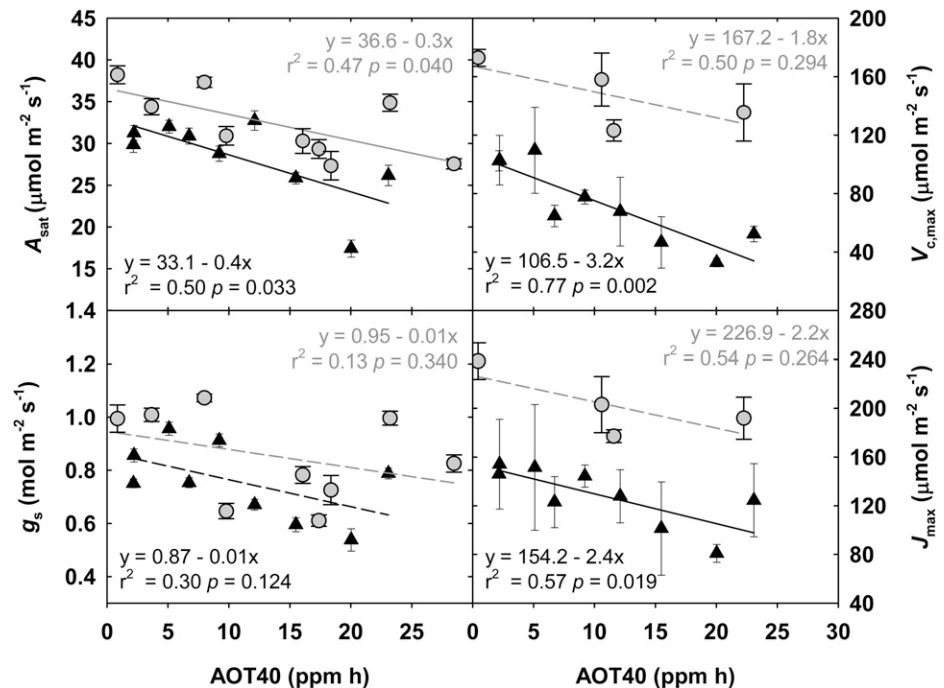


Table II. O_3 fumigation targets, exposures, and attainment for the nine 20-m-diameter plots in this experiment

AOT40 and SUM06 are season-long cumulative exposures, calculated according to Mauzerall and Wang (2001).

Target	24-h Mean	8-h Mean	1-h Mean (Maximum)	AOT40	SUM06	1-min Average within $\pm 20\%$ Target
				ppm h	ppm h	
2009						
Ambient	23.9	38.2	43.7	3.3	1.2	
40	24.8	40.8	46.5	3.8	1.2	81.8
55	29.7	47.6	56.1	9.0	5.9	76.2
70	29.9	56.1	67.7	16.8	33.8	83.9
85	32.9	61.1	81.0	21.0	36.4	77.1
110	38.5	74.0	91.4	31.4	48.4	79.2
130	45.3	93.1	113.8	47.2	67.9	79.9
160	47.5	99.5	126.7	52.9	71.0	74.4
200	54.6	120.6	153.8	67.4	85.6	67.0
2010						
Ambient	24.2	38.1	42.5	2.8	1.5	
55	28.6	46.2	48.6	12.0	16.8	80.6
70	29.4	54.0	63.6	14.2	27.7	83.7
85	35.1	61.4	72.6	20.6	34.7	82.1
110	37.3	72.9	92.2	30.2	46.4	83.3
130	41.4	80.7	104.6	38.7	55.5	74.7
150	37.7	75.4	100.6	33.1	45.0	67.4
170	42.6	90.7	124.0	45.8	61.9	60.1
190	47.2	90.5	128.7	46.3	60.1	53.6

August 27, 2010). When measured at this stage, Glc, Fru, Suc, starch, and protein showed significant negative linear responses to increasing O_3 exposure (Fig. 5). Total antioxidant capacity increased significantly with increasing O_3 in both years, and the leaf-level content of phenolic compounds increased significantly with increasing O_3 exposure in 2010 (Fig. 5). This suggests a tradeoff at the metabolite level for antioxidant metabolism versus primary metabolism.

On August 19, 2009, when seeds were filling, additional leaf tissue samples were taken for sugar alcohol, organic acid, and amino acid profiling. While 19

individual amino acids, three sugar alcohols, and numerous organic acids were individually identified by gas chromatography-mass spectrometry (GC-MS), this analysis focused on high-abundance and central metabolites. Pinitol, a common cyclitol in soybean associated with drought (Streeter et al., 2001), maltose, malate, which is the dicarboxylic acid that is a TCA cycle intermediate present in many cellular compartments (Martinoia and Rentsch, 1994), and total amino acids all showed negative linear responses to increasing chronic O_3 exposure (Fig. 5). Citrate, another TCA cycle intermediate, showed a positive linear trend in response to increasing O_3 exposure.

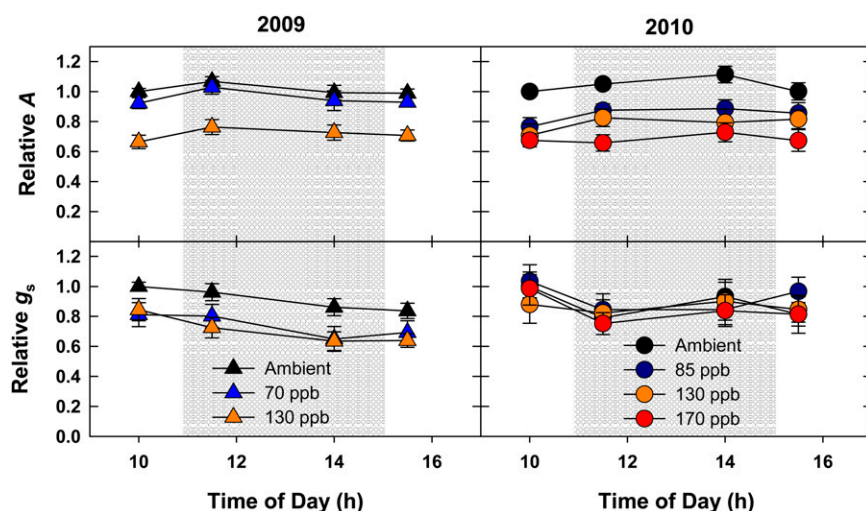
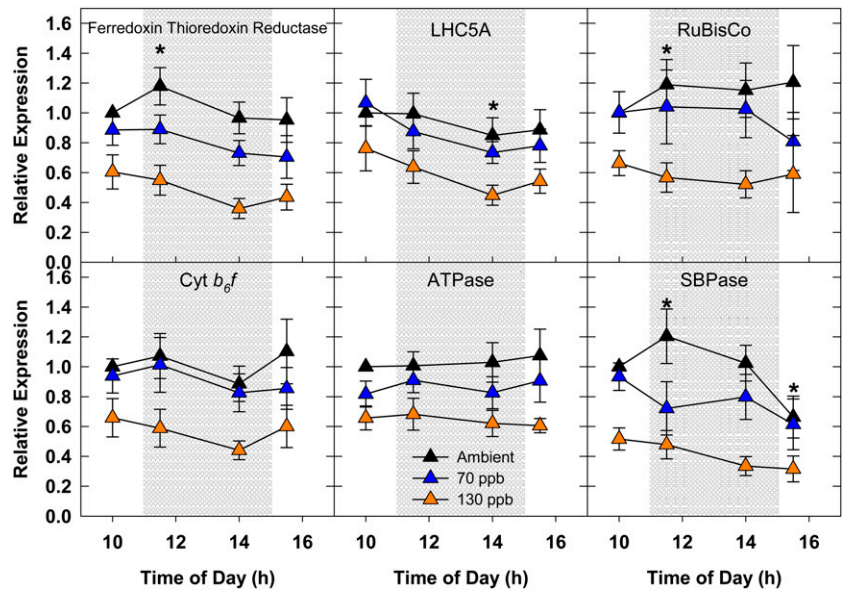


Figure 3. Season average diurnal gas exchange. Net assimilation and g_s were monitored before, during, and after the conclusion of O_3 fumigation in 2009 (black triangles) and 2010 (gray circles). Relative fold change values were calculated by comparing absolute values with the 10 AM ambient measurement. The shaded region signifies the period when O_3 was being fumigated. Error bars represent 95% confidence intervals.

Figure 4. Season average diurnal expression of select photosynthetic transcripts in 2009. Relative fold change values were calculated by comparing absolute values with the 10 AM ambient measurement. The shaded region signifies the period when O₃ was being fumigated. Error bars represent 95% confidence intervals. Asterisks indicate significant diurnal effects in transcript abundance for ambient-grown plants compared with the ambient 10 AM sampling time.



Linear Decrease in Seed Yield and Harvest Index with Increasing O₃ Concentration

Seed yield (Fig. 6, top panel) showed a significant negative correlation with elevated [O₃] in both 2009 and 2010. Despite differences in the fumigation treatments, average seasonal temperature, and rainfall between years, there was a consistent response of soybean seed yield to increasing [O₃], with a linear reduction of 37 to 39 kg ha⁻¹ per nL L⁻¹ cumulative O₃ exposure. The 100 seed weight (Fig. 6, middle panel) was significantly decreased in both 2009 and 2010 under elevated [O₃], although the response to elevated O₃ in 2010 was slightly less than in 2009. Harvest index (Fig. 6, bottom panel), the seed mass relative to standing total aboveground biomass, was significantly decreased under elevated [O₃] in 2009 and showed a negative trend in 2010. Like 100 seed weight, this response was slightly less in 2010 than in 2009.

DISCUSSION

This 2-year field study of soybean responses to a range of elevated [O₃] provides evidence that any increase in [O₃] above current concentrations will cause a significant decrease in seed yield. Across two growing seasons with different average seasonal temperature and rainfall patterns, there was a linear decrease in yield with increasing [O₃], at the rate of 37 to 39 kg ha⁻¹ per nL L⁻¹ cumulative exposure over 40 nL L⁻¹ (Fig. 6). This projection differs from earlier work at the Soybean Free Air Gas Concentration Enrichment (SoyFACE), where a single soybean genotype (Pioneer 93B15) was projected to lose 55 kg ha⁻¹ per nL L⁻¹ increase in [O₃] (Morgan et al., 2006), and the range of responses for six of the genotypes analyzed in this study was 18 to 30 kg ha⁻¹ per nL L⁻¹ cumulative exposure

over 40 nL L⁻¹ (Betzelberger et al., 2010). In our previous investigation of these cultivars, plants were exposed to a single elevated [O₃] (1.25–1.5 × ambient) in each of multiple years, and variation in that elevated O₃ target from year to year was used to construct dose-response curves (Betzelberger et al., 2010). However, variation in water availability, temperature, and pests or diseases could interact with the soybean response to O₃ (Booker et al., 2009; Ainsworth et al., 2012). Here, we investigated the O₃ exposure response of soybean under the same meteorological conditions each year, thus resulting in a more accurate estimate. Our results are very similar to the soybean O₃ exposure-response relationship estimated from the open-top chamber studies done in the 1980s and 1990s, recently reviewed by Mills et al. (2007). These results further substantiate the conclusion that the sensitivity of current soybean genotypes to O₃ is not different from early genotypes, despite the increasing background [O₃] during the intervening decades of soybean breeding (Betzelberger et al., 2010). These results also support the conclusion that the current range of concentrations experienced by soybean crops today is sufficient to exceed a critical threshold for O₃ damage (Mills et al., 2007).

Yield has been described as a function of available solar radiation and three main efficiencies: the ability of a crop canopy to intercept radiation (interception efficiency), the ability of plants to convert solar energy into carbohydrates (conversion efficiency), and the partitioning of that energy into seeds (partitioning efficiency; Monteith, 1977). Therefore, yield losses to stress can be analyzed in terms of stress effects on the seasonal distribution of leaf area and the ability of leaves to intercept radiation, the photosynthetic efficiency of leaves, and the ability of the plant to partition carbon to seeds. Based on 2 years of yield estimates

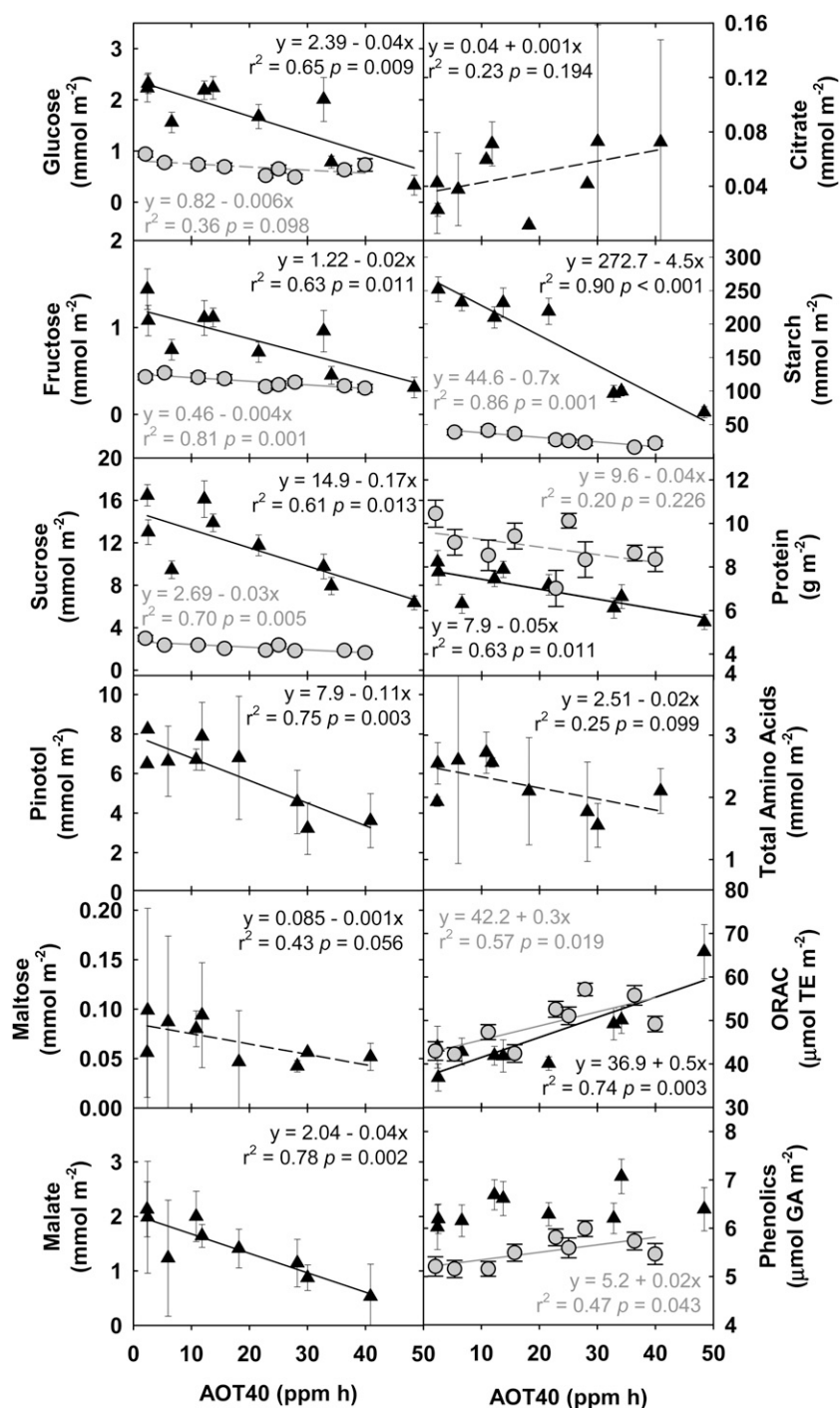


Figure 5. Linear regression of metabolites associated with primary metabolism, respiratory metabolism, and antioxidant capacity, which were measured during reproductive growth in 2009 (black triangles; R6, September 1, 2009) and 2010 (gray circles; R6, August 27, 2010). Solid lines indicate statistically significant relationships, while broken lines indicate trends. Error bars represent 95% confidence intervals.

from seven soybean genotypes, we found that increasing $[O_3]$ from ambient to a target concentration of 200 nL L^{-1} (AOT40 of 67.4 ppm h) reduced yields by 64% (Fig. 7). Harvest index, or the partitioning of carbon into seeds, was reduced by 12% over that range of $[O_3]$ (Fig. 7). Previous experiments at SoyFACE failed to resolve a significant effect of O_3 on harvest index (Morgan et al., 2006), and in this study, the decrease in harvest index by O_3 was only significant in

2009 (Fig. 6). Still, the average decline in harvest index with increasing $[O_3]$ across 2 years of study is similar to that reported previously for soybean (Leadley et al., 1990) and suggests that maintaining harvest index in elevated $[O_3]$ is one target for improving tolerance.

Interception efficiency is determined by the speed of canopy development and closure, leaf absorptance, canopy longevity, size, and architecture (Zhu et al., 2010). We estimated interception efficiency by adding

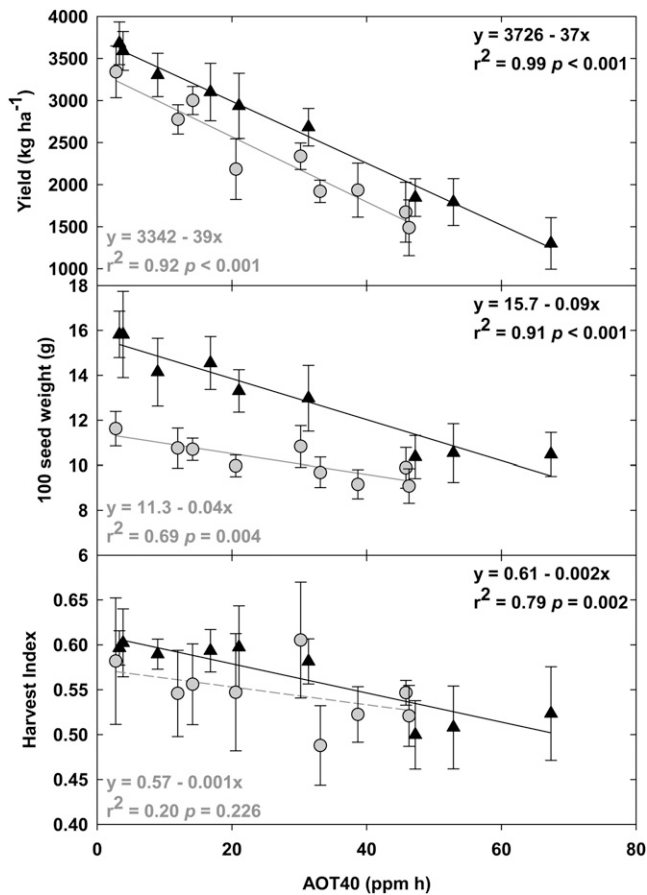


Figure 6. Linear regression of agronomic yield (top panel), 100 seed weight (middle panel), and harvest index (bottom panel) at the end of the growing season in 2009 (black triangles) and 2010 (gray circles). Solid lines indicate statistically significant relationships, while broken lines indicate trends. Error bars represent 95% confidence intervals.

the slope of the relative change in leaf absorbance to the slope of the relative change in season-long integrated LAI (Fig. 1). Based on this calculation, we estimate that exposure to the highest O₃ target of 200 nL L⁻¹ (AOT40 of 67.4 ppm h) may have decreased the potential interception efficiency by approximately 20% (Fig. 7). Increased reflectance and transmittance of leaves exposed to increasing [O₃] and subsequent decreased absorbance are common responses of leaves to O₃ and other stresses associated with reduced leaf chlorophyll concentration (Carter et al., 1995; Carter and Knapp, 2001). In addition to changes in leaf-level properties, functional LAI significantly decreased with increasing [O₃] (Fig. 1), and a reduction in LAI at the highest [O₃] was apparent after approximately 4 weeks of exposure (data not shown). Toward the end of the growing season, a senescence-induced reduction in LAI occurred approximately 2 weeks earlier in the highest [O₃]. Thus, both the duration and the size of the canopy were significantly affected by O₃ in this study. In previous studies, changes in soybean canopy light interception with increasing exposure to O₃ were

small or nonexistent (Unsworth et al., 1984; Leadley et al., 1990; Dermody et al., 2008). The maximum LAI of 4 to 6 units measured in this study was much less than that reported in previous studies, where LAI was greater than 10 (Unsworth et al., 1984; Leadley et al., 1990). Furthermore, the O₃ concentrations used in this study were greater than previous studies at SoyFACE (Dermody et al., 2008). Thus, our interpretation differs from previous studies, and these data suggest that increasing [O₃] can significantly impact canopy interception efficiency.

Genotypes in different maturity groups (II, III, and IV) were equally O₃ sensitive in this study, and elevated [O₃] consistently decreased leaf longevity. Therefore, a potential strategy for improving soybean yield in elevated [O₃] may be to counteract the acceleration of senescence. Delayed leaf senescence was a notable phenotype of high-yielding transgenic soybean lines expressing an Arabidopsis B-box domain gene (Preuss et al., 2012), which demonstrates the potential for improving productivity by delaying senescence.

The efficiency of soybean to convert solar energy into biomass energy is also negatively impacted by O₃ (Fig. 7; Leadley et al., 1990; Fiscus et al., 2005; Dermody et al., 2008; Gillespie et al., 2012). Conversion efficiency is the combined gross photosynthesis of all leaves within the canopy minus respiratory losses of carbon (Zhu et al., 2010). O₃ negatively impacts conversion efficiency by reducing photosynthetic efficiency and by increasing respiratory costs (Skarby et al., 1987; Amthor, 1988; Dizengremel et al., 2008; Gillespie et al., 2012). The conversion efficiency of a canopy is typically estimated by plotting the accumulated dry biomass versus the cumulative intercepted radiation and fitting a slope to that line (Dohleman and Long, 2009). In this study, we were limited by the size of the cultivar plots and could

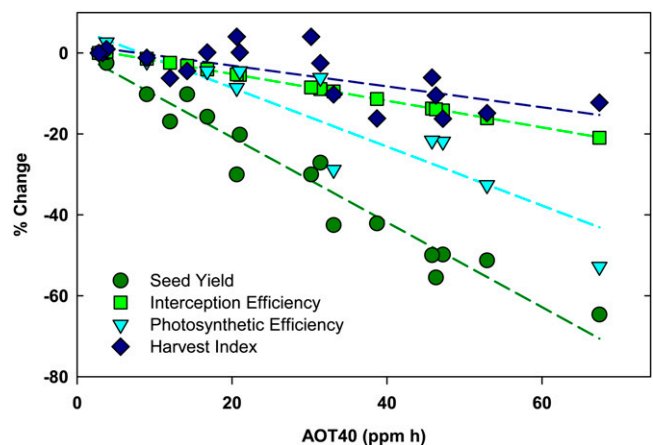


Figure 7. Parameterization of yield loss (circles) as accumulated losses in light interception efficiency (squares), conversion efficiency (triangles), and partitioning efficiency (harvest index; diamonds) under elevated O₃. Data from 2009 and 2010 were combined for these regressions.

not do destructive biomass harvests during the growing season. Instead, we conservatively estimated the effects of O_3 on potential conversion efficiency by plotting photosynthetic efficiency as the relative change in photosynthetic capacity ($V_{c,max}$) with increasing O_3 exposure. Based on this calculation, photosynthetic efficiency decreased by 41% from ambient to the highest $[O_3]$ (Fig. 7). This is likely an underestimate of the potential effects of O_3 on conversion efficiency, because the increased respiration costs (Gillespie et al., 2012) are not taken into account. Still, the large decrease in photosynthetic efficiency relative to changes in harvest index and interception efficiency (Fig. 7) agree with previous studies, indicating that the effect of O_3 on conversion efficiency is an important contributor to yield loss (Unsworth et al., 1984; Leadley et al., 1990; Dermody et al., 2008).

Lower maximum Rubisco activity and lower maximum electron transport capacity (Fig. 2) lead to decreased rates of A and g_s at higher $[O_3]$, which were also associated with lower levels of transcript abundance of genes encoding photosynthetic proteins (Fig. 4). A recent proteomics experiment investigating the timing of changes in thylakoid proteins to O_3 exposure showed decreased abundance of most proteins within 14 d of exposure to O_3 (Bohler et al., 2011), consistent with the transcriptional changes reported here. Previous work at this site also demonstrated that oxidation of Rubisco protein was significantly greater in plants exposed to elevated $[O_3]$ (Galant et al., 2012). In this study, the decrease in photosynthetic metabolism fed forward to alter leaf contents of sugars, sugar alcohols, and starch. While interpreting metabolite profiles is complicated by a number of issues (Fernie and Stitt, 2012), in general, there was a negative linear trend in metabolite content with increasing O_3 exposure (Fig. 5). While other studies have reported increased Suc content with exposure to elevated $[O_3]$ (Britz and Robinson, 2001), the decline in the Suc content with increasing $[O_3]$ in this study is consistent with previously reported decreases in Suc synthesis activity and increased Suc breakdown (invertase activity) in O_3 -sensitive common bean (*Phaseolus vulgaris*) lines (Guidi et al., 2009). There was also a trend toward an increase in citrate content with increasing $[O_3]$. This trend is consistent with the hypothesis that O_3 increases the activity of phosphoenolpyruvate carboxylase (Dizengremel et al., 2009), which then supplies the TCA cycle and mitochondrial respiration with carbon (Dizengremel et al., 2012).

It has been previously reported that elevated $[O_3]$ increases respiration rates in soybean and the total antioxidant capacity of soybean leaves (Gillespie et al., 2012). Here, we further demonstrate that the increase in total antioxidant capacity of leaves is linearly related to O_3 exposure. An additional source of respiratory carbon loss is related to the enhanced deposition of epicuticular wax that is induced by elevated $[O_3]$ (Percy et al., 2009). Scanning electron microscopy revealed that 130 nL L^{-1} $[O_3]$ caused noticeable

increases in the amount of wax deposited to the abaxial leaf epidermal surface (Supplemental Fig. S2). Furthermore, the rate of chlorophyll leached from the leaves of plants grown in elevated O_3 was decreased (Supplemental Fig. S2), which is consistent with increased epicuticular wax content (Raffaele et al., 2008; Samuels et al., 2008).

CONCLUSION

Nearly 40% of the world's soybean production occurs in the midwest United States, where current $[O_3]$ ranges from 40 to 60 nL L^{-1} during the summer growing season. As demonstrated in this field study, these concentrations are sufficient to significantly reduce yields. Seven soybean cultivars showed very similar responses to a range of O_3 , indicating the general sensitivity of this crop to O_3 pollution. The fact that the efficiency of light interception, the efficiency of converting solar energy into biomass, and the harvest index were all detrimentally impacted by increasing $[O_3]$ suggests that there are multiple avenues for improving soybean responses to this stress.

MATERIALS AND METHODS

Experimental Site and Plant Growth Conditions

The SoyFACE facility is located on 32 ha near Champaign, Illinois (40° 02'N, 88°14'W, 228 m above sea level; <http://www.igb.illinois.edu/soyface/>). Soybean (*Glycine max*) and maize (*Zea mays*) are each planted on one-half of the area and rotated annually. In 2009 and 2010, seven indeterminate soybean cultivars (Table I) were planted in plots eight rows wide and 5.4 m long, with 0.38-m row spacing. Planting dates were June 9, 2009, and May 27, 2010. O_3 fumigation began on June 29, 2009, and June 6, 2010, and ended on September 27, 2009, and September 17, 2010. Meteorological data, including PPFD (Supplemental Fig. S1, A and B), air temperature (Supplemental Fig. S1, C and D), rainfall (Supplemental Fig. S1, E and F), and ambient $[O_3]$ (Supplemental Fig. S3) were measured throughout the two growing seasons.

In this experiment, eight 20-m-diameter SoyFACE plots were exposed to different O_3 concentrations (Table II). The fumigation system, based on the design of Miglietta et al. (2001), added air enriched with O_3 to maintain a set concentration for each plot for approximately 8 h each day. Fumigation targets, average and cumulative exposures, and attainment information for the SoyFACE plots are shown in Table II. The AOT40 and the sum of hourly O_3 greater than or equal to 60 nL L^{-1} (SUM06) were calculated for the entire growing season (Mauzerall and Wang, 2001).

LAI, Relative Chlorophyll Content, and Leaf Absorptance

LAI was measured weekly on all seven cultivars throughout the 2009 and 2010 growing seasons, as described by Betzelberger et al. (2010), with a plant canopy analyzer (LAI-2000; Li-Cor) that calculates LAI using a fish-eye optical sensor that measures radiation attenuation through the canopy (Welles and Norman, 1991). Weekly, relative chlorophyll content was measured on three fully expanded leaves at the top of the canopy within each cultivar of each plot with a SPAD meter (Minolta SPAD-502). SPAD values were then converted to chlorophyll content by an exponential function, $y = 0.089e^{(0.0411x)}$, where y is the chlorophyll content ($g\ m^{-2}$) and x is the SPAD reading, which was experimentally determined for these genotypes by Betzelberger et al. (2010).

Two leaves from each cultivar per plot were sampled for absorptance measurements. On August 17, 2009, four cultivars, Dwight, IA-3010, LN97-15076, and Pana, were sampled from ambient, 70, and 130 nL L^{-1} plots. On August 17, 2010, those four cultivars were sampled from ambient, 85, 130, and 170 nL L^{-1} plots. Leaf reflectance and transmittance from 400 to 700 nm were

measured on all three trifoliates using an integrating sphere (LI 1800, Li-Cor) and a miniature fiber optic spectroradiometer (USB2000; Ocean Optics). Leaf absorbance was calculated as $1 - \text{reflectance} - \text{transmittance}$.

Photosynthetic Gas Exchange and Chlorophyll Fluorescence

Midday photosynthetic gas exchange and chlorophyll fluorescence of fully expanded leaves at the top of the canopy were measured four times during the growing season: during vegetative growth (V4 on June 27, 2009, and V5 on June 28, 2010), full bloom (R2 on July 27, 2009, and R2 on July 14, 2010), beginning of seed formation (R4 on August 10, 2009, and R4 on July 28, 2010), and full seed stage (R6 on September 1, 2009, and R6 on August 27, 2010). Measurements were made using four to six open gas-exchange systems with integrated modulated chlorophyll fluorometers (LI-6400 and LI-6400-40; Li-Cor). Measurements were made on three plants in each cultivar subplot within each experimental O₃ plot. Measurements of chlorophyll fluorescence and gas exchange were made at ambient [CO₂] (approximately 390 $\mu\text{L L}^{-1}$), ambient air temperature, and incident photosynthetically active photon flux. Leaf photosynthesis (A), g_s to water vapor, and intercellular CO₂ concentration (c_i) were calculated using the equations of Von Caemmerer and Farquhar (1981). The photochemical efficiency of PSII was determined by measuring steady-state fluorescence and maximum fluorescence during a light-saturating pulse of approximately 6,500 $\mu\text{mol m}^{-2} \text{s}^{-1}$ following the procedures of Genty et al. (1989).

Diurnal measurements of photosynthesis were made before and after the initiation of fumigation on four separate days in 2009 (July 14, July 30, August 14, and August 25) and twice in 2010 (July 2 and July 26) on Dwight, IA-3010, LN97-15076, and Pana to investigate the immediate effects on O₃ on leaf physiology. Gas exchange was measured in the field on three leaves per cultivar as described above before the O₃ fumigation was turned on, approximately 10 to 30 min after fumigation was initiated, approximately 5 h after fumigation was on, and approximately 10 to 30 min after the fumigation was turned off. On these days, O₃ fumigation was adjusted to begin at 11 AM and end at 3 PM. Immediately following gas exchange, leaf tissue was collected for RNA isolation by immediately freezing in liquid N.

The response of A to changes in c_i was measured under saturating or near-saturating light (1,500–2,000 $\mu\text{mol m}^{-2} \text{s}^{-1}$) on four occasions in 2009 (R1 July 17, R2 July 28, R4 August 5, R5 August 19; Fig. 2) and one occasion in 2010 (R3 July 25; Fig. 2). Three leaves per cultivar per O₃ plot were measured. In 2009, Dwight and IA-3010 were measured, and in 2010, Dwight, IA-3010, LN97-15076, and Pana were measured. Measurements were taken in the laboratory on leaves cut, under water, before dawn on the day that they were measured. This ensured that the A/c_i responses reflected the potential photosynthesis on the day of measurement and were not affected by transient decreases that may result during the day due to photoinhibition, water stress, or feedback inhibition due to carbohydrate accumulation and cytosolic inorganic phosphate limitation (Long and Bernacchi, 2003). The $V_{c,\text{max}}$ and the J_{max} were calculated by fitting the equations of Farquhar et al. (1980).

Tissue Sampling, and Biochemical and Molecular Analyses

Leaf tissue samples for measuring total antioxidant capacity, phenolic content, hexose, Suc and starch contents, and specific leaf mass were taken immediately following midday photosynthesis measurements in 2009 and 2010. Leaf discs (approximately 1.4 cm²) were excised from fully expanded leaves at the top of the canopy, plunged immediately into liquid nitrogen, and then stored at -80°C . Five plants per cultivar per plot were sampled for total antioxidant capacity measurements and for oven drying at 70°C for calculation of specific leaf mass. Three plants per cultivar per plot were sampled for determination of phenolic content and carbohydrate content.

Total antioxidant capacity was assessed with the oxygen radical absorbance capacity assay, which measures antioxidant inhibition of peroxyl radical-induced oxidations, according to the methods of Gillespie et al. (2007). Total phenolic content was measured with a Folin-Ciocalteu assay (Ainsworth and Gillespie, 2007). Total carbohydrate content was calculated from the sequential determination of Glc, Fru, and Suc contents using the methods of Jones et al. (1977). The pellets of this ethanol extraction were then solubilized by heating to 95°C in 0.1 M NaOH for determination of protein and starch contents. Protein content was determined using a commercial protein assay kit (Pierce) with bovine serum albumin as a standard. The NaOH solution was then

acidified to pH 4.9, and starch content was determined from Glc equivalents (Hendriks et al., 2003).

Chlorophyll loss was monitored over time by placing an intact center trifoliolate in 50 mL of ethanol (96%, v/v). At the specified times, 200 μL of extract was collected and measured at 470, 649, and 665 nm using a spectrophotometer (Synergy 2 Multi-Mode Microplate Reader; BioTek Instruments) to quantify chlorophyll content using the formulas of Porra et al. (1989). Leaflets were then kept in ethanol overnight in order to determine total chlorophyll content.

On August 19, 2009, when seeds were filling, three additional leaf discs (approximately 2 cm²) from two cultivars (Dwight and IA-3010) per O₃ plot were sampled for sugar and amino acid profiling using GC-MS. Samples were extracted with 80% (v/v) ethanol several times until the leaf discs were colorless. The ethanol-soluble fractions from each sample were pooled and frozen at -20°C for subsequent analysis. For sugar analysis, various amounts of individual standard solutions were used to prepare calibration curves ranging from 0.3 to 75 μg in the autosample vials, and a composite standard was also prepared, varying from 50 to 150 nmol (1–40 μg). The sample and standard aliquots were dried in 1.5-mL autosampler vials in a SpeedVac concentrator at 55°C under vacuum and then converted to their oxime derivatives using a pyridine solution containing 12.5 mg mL⁻¹ hydroxylamine hydrochloride and 90 $\mu\text{g mL}^{-1}$ phenyl- β -D-glucopyranoside. Phenyl- β -D-glucopyranoside was used as the internal standard. Hydroxylamine converted carbonyl compounds to their oxime derivatives to prevent amination, thus reducing the number of peaks for simplicity. Samples were mixed by vortex and incubated at 70°C for 40 min with occasional mixing. After cooling, hexamethyldisilazane (HMDS) was added. Then, samples were allowed to react for 60 min at room temperature. Trifluoroacetic acid was used in this method to remove any traces of water in the sample, as HMDS is sensitive to water vapor. HMDS selectively silylates carbohydrates into their trimethyl silyl sugar derivatives and provides simpler chromatograms than bis(trimethylsilyl)trifluoroacetamide.

Trimethyl silyl sugar derivatives were separated on a DB-1701 capillary column (30 m \times 0.25 mm i.d., with a 0.25- μm film thickness; Supelco) using an Agilent 6890N gas chromatograph system and detected with an Agilent 5975B insert MS detector (Agilent Technologies). The detector temperature was 230°C , and the injector temperature was 250°C . The initial column temperature of 120°C was held for 3 min and then increased to 170°C at a rate of $20^\circ\text{C min}^{-1}$, then to 200°C at a rate of 4°C min^{-1} , and finally to 280°C at a rate of 6°C min^{-1} , which was maintained for 5 min. The carrier gas was helium at a flow rate of 1.3 mL min⁻¹. The mass spectrometer was operated in the electron-impact mode with an ionization energy of 70 eV. The scan range was set from 50 to 650 D. Compound identification was performed by comparison with the chromatographic retention characteristics and mass spectra of authentic standards, reported mass spectra, and the mass spectral library of the GC-MS data system. Standard mixtures of known reference compounds were run side by side with the soybean samples each day. Compounds were quantified using total ion current peak area and converted to compound mass using calibration curves of external and internal standards.

Free amino acids were derived using the EZ:faast free amino acid analysis kit (Phenomenex) according to the manufacturer's instructions. Amino acid derivatives were separated on a ZB-AAA GC capillary column (10 m \times 0.18 mm i.d., with a 0.18- μm film thickness; Phenomenex) using an Agilent 6890N gas chromatograph system and detected with Agilent 5975B insert MS detector (Agilent Technologies). The MS temperatures were as follows: ion source, 240°C ; quadrupole, 180°C ; and auxiliary, 310°C . The injector temperature was 250°C . The initial column temperature of 110°C was held for 1 min and then ramped at a rate of $30^\circ\text{C min}^{-1}$ to 320°C , which was held for 1 min. The carrier gas was helium at a flow rate of 1.1 mL min⁻¹. The mass spectrometer was operated in the electron-impact mode with an ionization energy of 70 eV. The scan range was set from 43 to 450 mass-to-charge ratio. A 2- μL sample was injected in the split mode (1:15, v/v). Compound identification was performed by comparison with the chromatographic retention characteristics and mass spectra of authentic standards, reported mass spectra, and the mass spectral library of the GC-MS data system. Standard mixtures of known reference compounds were run side by side with the soybean samples, and compounds were quantified using total ion current peak area as described above.

Scanning Electron Microscopy

Leaf tissue was collected on August 31, 2009 by taking leaf punches from the center trifoliolate halfway between the petiole and the leaf tip and halfway between the leaf edge and the midvein from the same leaves that were sampled for gas exchange on August 25, 2009. The leaf sections were fixed in 4% formaldehyde, 50 mM PIPES, pH 6.8, by vacuum infiltration for 20 min. The tissue

was dehydrated using a graded series of ethanol in water (25%, 50%, 75%, and 100% [v/v] ethanol:water). Leaf sections were then critical point dried in liquid CO₂, affixed to 2.7-cm-diameter stubs using conductive carbon paint, and sputter coated with gold/palladium for 90 s. Surface images were taken on a 6060LV scanning electron microscope (JEOL USA). Each leaf section was viewed at 500× and 2,000× to obtain images of the abaxial epidermis.

Quantitative Reverse Transcription-PCR

RNA was isolated as described by Bilgin et al. (2009), and RNA quality was verified on a 1% agarose gel. One microgram of DNase-treated RNA (TURBO DNA-free kit; Life Technologies) was used as a template for first-strand complementary DNA synthesis using SuperScript II (Life Technologies) and oligo(dT) primers (Life Technologies). A 10-μL reaction using Power SYBR Green PCR master mix (Life Technologies) and 400 nM of each primer was performed on the 7900HT Fast Real-Time PCR System (Life Technologies). An automated liquid-handling system (JANUS; Perkin-Elmer) was used to aliquot primers onto a 384-well PCR plate. The following sequences were used as primers for each of the target genes: FTR (Glyma13g04640 forward, 5'-TACGCCCGTAAGTCAGGAAC-3'; Glyma13g04640 reverse, 5'-AATCCTTGCAACCTCAGC-3'), LHC5A (Glyma06g04280 forward, 5'-GTGGAGCATCTTTCCAATCC-3'; Glyma06g04280 reverse, 5'-TGGATAAGCTCAAGCCCAAG-3'), Cyt b6f (Glyma06g03920 forward, 5'-CCCGACAAGAACAAGTCCAT-3'; Glyma06g03920 reverse, 5'-CAGTGAAGCAGCAACATCAA-3'), ATPase (Glyma13g23260 forward, 5'-ATTTGCTCAGGCCATTTGTT-3'; Glyma13g23260 reverse, 5'-AGGTTGCAGTTGAAGACAGC-3'), Rubisco small subunit (Glyma19g06340 forward, 5'-GCACAATTGGCAAAGGAAGT-3'; Glyma19g06340 reverse, 5'-GAGAAGCATCAGTGCAACCA-3'), and SBPase (Glyma11g34900 forward, 5'-ATAAGTTGACCGGCATCACC-3'; Glyma11g34900 reverse, 5'-GGGTTGTCAGATGTGGCTCT-3'). The PCR efficiency and threshold value for each PCR amplification curve were determined using LinRegPCR software (Ruijter et al., 2009) by analyzing the baseline-corrected ΔRn (Rn – baseline) values in the log-linear phase. The normalized expression level for each target was calculated as reported by Gillespie et al. (2011) using cons6 and cons15 (Libault et al., 2008) as endogenous controls. Relative expression was calibrated to the 10 AM ambient sample.

Harvest

At harvest maturity, the cultivar plots were trimmed to 4.9 m in length and the center six rows were harvested on October 20, 2009 (DOY 293), and September 30, 2010 (DOY 273). In both years, yield and seed composition measurements were made on 11.2-m² final harvest plots. Seed yield, 100 seed weight, and harvest index were assessed by harvesting five plants per cultivar within each octagonal plot in 2009 and 10 plants per cultivar in 2010. All shoot dry mass was harvested by hand and separated into reproductive and vegetative material. The ratio of total seed weight to the total aboveground dry weight biomass per plant at maturity (minus leaves) was used to determine harvest index per plant and then averaged to determine plot mean harvest index in both years.

Statistical Analysis

Regression analysis was performed on plot means for all variables. Mean values for all cultivars ± 95% confidence intervals based on the number of cultivars sampled at each time point are presented in all figures. Linear regression was used to analyze the associations between O₃ exposure and each measured variable (SAS Institute; SigmaPlot, Systat Software). Transcript levels were analyzed by individual Student's *t* tests against the relative expression level in ambient [O₃] at the 10 AM time point.

Supplemental Data

The following materials are available in the online version of this article.

Supplemental Figure S1. Meteorological data measured in 2009 and 2010.

Supplemental Figure S2. Abaxial surface of leaves grown in ambient and elevated [O₃].

Supplemental Figure S3. O₃ concentration measured throughout the two growing seasons.

ACKNOWLEDGMENTS

We thank current and previous SoyFACE managers Tim Mies, Charlie Mitsdarfer, Kannan Puthuval, Chris Montes, and David Drag, David Rosenthal, Bob Koester, Courtney Leisner, Jeff Skoneczka, Joe Sullivan, Payam Vatani, Sara Kammlade, Cody Markelz, Sharon Gray, Katie Richter, Matt Siebers, and Reid Strellner provided assistance with gas exchange and sampling at SoyFACE.

Received August 16, 2012; accepted October 3, 2012; published October 4, 2012.

LITERATURE CITED

- Ainsworth EA, Gillespie KM (2007) Estimation of total phenolic content and other oxidation substrates in plant tissues using Folin-Ciocalteu reagent. *Nat Protoc* 2: 875–877
- Ainsworth EA, Yendrek CR, Sitch S, Collins WJ, Emberson LD (2012) The effects of tropospheric ozone on net primary productivity and implications for climate change. *Annu Rev Plant Biol* 63: 637–661
- Amthor JS (1988) Growth and maintenance respiration in leaves of bean (*Phaseolus vulgaris* L.) exposed to ozone in open-top chambers in the field. *New Phytol* 110: 319–325
- Ashmore M, Emberson L, Karlsson PE, Pleijel H (2004) New directions: a new generation of ozone critical levels for the protection of vegetation in Europe. *Atmos Environ* 38: 2213–2214
- Avnery S, Mauzerall DL, Liu J, Horowitz LW (2011a) Global crop yield reductions due to surface ozone exposure. 1. Year 2000 crop production losses and economic damage. *Atmos Environ* 45: 2284–2296
- Avnery S, Mauzerall DL, Liu J, Horowitz LW (2011b) Global crop yield reductions due to surface ozone exposure. 2. Year 2030 potential crop production losses and economic damage under two scenarios of O₃ pollution. *Atmos Environ* 45: 2297–2309
- Bernacchi CJ, Leakey ADB, Heady LE, Morgan PB, Dohleman FG, McGrath JM, Gillespie KM, Wittig VE, Rogers A, Long SP, et al (2006) Hourly and seasonal variation in photosynthesis and stomatal conductance of soybean grown at future CO₂ and ozone concentrations for 3 years under fully open-air field conditions. *Plant Cell Environ* 29: 2077–2090
- Betzelberger AM, Gillespie KM, McGrath JM, Koester RP, Nelson RL, Ainsworth EA (2010) Effects of chronic elevated ozone concentration on antioxidant capacity, photosynthesis and seed yield of 10 soybean cultivars. *Plant Cell Environ* 33: 1569–1581
- Bilgin DD, DeLucia EH, Clough SJ (2009) A robust plant RNA isolation method suitable for Affymetrix GeneChip analysis and quantitative real-time RT-PCR. *Nat Protoc* 4: 333–340
- Bohler S, Sergeant K, Hoffmann L, Dizengremel P, Hausman J-F, Renaut J, Jolivet Y (2011) A difference gel electrophoresis study on thylakoids isolated from poplar leaves reveals a negative impact of ozone exposure on membrane proteins. *J Proteome Res* 10: 3003–3011
- Booker F, Muntifering R, McGrath M, Burkey K, Decoteau D, Fiscus E, Manning W, Krupa S, Chappelka A, Grantz D (2009) The ozone component of global change: potential effects on agricultural and horticultural plant yield, product quality and interactions with invasive species. *J Integr Plant Biol* 51: 337–351
- Britz SJ, Robinson JM (2001) Chronic ozone exposure and photosynthate partitioning into starch in soybean leaves. *Int J Plant Sci* 162: 111–117
- Carter GA, Knapp AK (2001) Leaf optical properties in higher plants: linking spectral characteristics to stress and chlorophyll concentration. *Am J Bot* 88: 677–684
- Carter GA, Rebbeck J, Percy KE (1995) Leaf optical properties in *Liriodendron tulipifera* and *Pinus strobus* as influenced by increased atmospheric ozone and carbon dioxide. *Can J Res* 25: 407–412
- Chen CP, Frank TD, Long SP (2009) Is a short, sharp shock equivalent to long-term punishment? Contrasting the spatial pattern of acute and chronic ozone damage to soybean leaves via chlorophyll fluorescence imaging. *Plant Cell Environ* 32: 327–335
- Dermody O, Long SP, McConnaughey K, DeLucia EH (2008) How do elevated CO₂ and O₃ affect the interception and utilization of radiation by a soybean canopy? *Glob Change Biol* 14: 556–564
- Dizengremel P, Le Thiec D, Bagard M, Jolivet Y (2008) Ozone risk assessment for plants: central role of metabolism-dependent changes in reducing power. *Environ Pollut* 156: 11–15

- Dizengremel P, Le Thiec D, Hasenfratz-Sauder MP, Vaultier MN, Bagard M, Jolivet Y (2009) Metabolic-dependent changes in plant cell redox power after ozone exposure. *Plant Biol (Stuttg)* (Suppl 1) **11**: 35–42
- Dizengremel P, Vaultier M-N, Le Thiec D, Cabané M, Bagard M, Gérant D, Gérard J, Dghim AA, Richet N, Affif D, et al (2012) Phosphoenolpyruvate is at the crossroads of leaf metabolic responses to ozone stress. *New Phytol* **195**: 512–517
- Dohleman FG, Long SP (2009) More productive than maize in the Midwest: how does *Miscanthus* do it? *Plant Physiol* **150**: 2104–2115
- Emberson LD, Ashmore MR, Cambridge HM, Simpson D, Tuovinen JP (2000) Modelling stomatal ozone flux across Europe. *Environ Pollut* **109**: 403–413
- Emberson LD, Bueker P, Ashmore MR, Mills G, Jackson LS, Agrawal M, Atikuzzaman MD, Cinderby S, Engardt M, Jamir C, et al (2009) A comparison of North American and Asian exposure-response data for ozone effects on crop yields. *Atmos Environ* **43**: 1945–1953
- Fares S, Park J-H, Ormeno E, Gentner DR, McKay M, Loreto F, Karlik J, Goldstein AH (2010) Ozone uptake by citrus trees exposed to a range of ozone concentrations. *Atmos Environ* **44**: 3404–3412
- Farquhar GD, Caemmerer SV, Berry JA (1980) A biochemical-model of photosynthetic CO₂ assimilation in leaves of C₃ species. *Planta* **149**: 78–90
- Fernie AR, Stitt M (2012) On the discordance of metabolomics with proteomics and transcriptomics: coping with increasing complexity in logic, chemistry, and network interactions scientific correspondence. *Plant Physiol* **158**: 1139–1145
- Fiscus EL, Booker FL, Burkey KO (2005) Crop responses to ozone: uptake, modes of action, carbon assimilation and partitioning. *Plant Cell Environ* **28**: 997–1011
- Fuhrer J, Skärby L, Ashmore MR (1997) Critical levels for ozone effects on vegetation in Europe. *Environ Pollut* **97**: 91–106
- Gadjev I, Vanderauwera S, Gechev TS, Laloi C, Minkov IN, Shulaev V, Apel K, Inzé D, Mittler R, Van Breusegem F (2006) Transcriptomic footprints disclose specificity of reactive oxygen species signaling in Arabidopsis. *Plant Physiol* **141**: 436–445
- Galant A, Koester RP, Ainsworth EA, Hicks LM, Jez JM (2012) From climate change to molecular response: redox proteomics of ozone-induced responses in soybean. *New Phytol* **194**: 220–229
- Genty B, Briantais JM, Baker NR (1989) The relationship between the quantum yield of photosynthetic electron-transport and quenching of chlorophyll fluorescence. *Biochim Biophys Acta* **990**: 87–92
- Gillespie KM, Chae JM, Ainsworth EA (2007) Rapid measurement of total antioxidant capacity in plants. *Nat Protoc* **2**: 867–870
- Gillespie KM, Rogers A, Ainsworth EA (2011) Growth at elevated ozone or elevated carbon dioxide concentration alters antioxidant capacity and response to acute oxidative stress in soybean (*Glycine max*). *J Exp Bot* **62**: 2667–2678
- Gillespie KM, Xu F, Richter KT, McGrath JM, Markelz RJC, Ort DR, Leakey ADB, Ainsworth EA (2012) Greater antioxidant and respiratory metabolism in field-grown soybean exposed to elevated O₃ under both ambient and elevated CO₂. *Plant Cell Environ* **35**: 169–184
- Goumenaki E, Taybi T, Borland A, Barnes J (2010) Mechanisms underlying the impacts of ozone on photosynthetic performance. *Environ Exp Bot* **69**: 259–266
- Guidi L, Degl'Innocenti E, Martinelli F, Piras M (2009) Ozone effects on carbon metabolism in sensitive and insensitive *Phaseolus* cultivars. *Environ Exp Bot* **66**: 117–125
- Heagle AS (1989) Ozone and crop yield. *Annu Rev Phytopathol* **27**: 397–423
- Hendriks JHM, Kolbe A, Gibon Y, Stitt M, Geigenberger P (2003) ADP-glucose pyrophosphorylase is activated by posttranslational redox-modification in response to light and to sugars in leaves of Arabidopsis and other plant species. *Plant Physiol* **133**: 838–849
- Jones MGK, Outlaw WH, Lowry OH (1977) Enzymic assay of 10⁻⁷ to 10⁻¹⁴ moles of sucrose in plant tissues. *Plant Physiol* **60**: 379–383
- Kangasjärvi J, Jaspers P, Kollist H (2005) Signalling and cell death in ozone-exposed plants. *Plant Cell Environ* **28**: 1021–1036
- Kollist T, Moldau H, Rasulov B, Oja V, Rämme H, Hüve K, Jaspers P, Kangasjärvi J, Kollist H (2007) A novel device detects a rapid ozone-induced transient stomatal closure in intact Arabidopsis and its absence in abi2 mutant. *Plant Physiol* **129**: 796–803
- Leadley PW, Reynolds JF, Flagler R, Heagle AS (1990) Radiation utilization efficiency and the growth of soybeans exposed to ozone: a comparative analysis. *Agric For Meteorol* **51**: 293–308
- Libault M, Thibivilliers S, Bilgin DD, Radwan O, Benitez M, Clough SJ, Stacey G (2008) Identification of four soybean reference genes for gene expression normalization. *Plant Genome* **1**: 44–54
- Long SP, Bernacchi CJ (2003) Gas exchange measurements, what can they tell us about the underlying limitations to photosynthesis? Procedures and sources of error. *J Exp Bot* **54**: 2393–2401
- Martinoia E, Rentsch D (1994) Malate compartmentation: responses to complex metabolism. *Annu Rev Plant Physiol Plant Mol Biol* **45**: 447–467
- Mauzerall DL, Wang XP (2001) Protecting agricultural crops from the effects of tropospheric ozone exposure: reconciling science and standard setting in the United States, Europe, and Asia. *Annu Rev Energy Environ* **26**: 237–268
- Miglietta F, Peressotti A, Vaccari FP, Zaldei A, deAngelis P, Scarascia-Mugnozza G (2001) Free-air CO₂ enrichment (FACE) of a poplar plantation: the PopFACE fumigation system. *New Phytol* **150**: 465–476
- Mills G, Buse A, Gimeno B, Bermejo V, Holland M, Emberson L, Pleijel H (2007) A synthesis of AOT40-based response functions and critical levels of ozone for agricultural and horticultural crops. *Atmos Environ* **41**: 2630–2643
- Monteith JL (1977) Climate and efficiency of crop production in Britain. *Philos Trans R Soc B* **281**: 277–294
- Morgan PB, Ainsworth EA, Long SP (2003) How does elevated ozone impact soybean? A meta-analysis of photosynthesis, growth and yield. *Plant Cell Environ* **26**: 1317–1328
- Morgan PB, Mies TA, Bollero GA, Nelson RL, Long SP (2006) Season-long elevation of ozone concentration to projected 2050 levels under fully open-air conditions substantially decreases the growth and production of soybean. *New Phytol* **170**: 333–343
- Overmyer K, Brosché M, Kangasjärvi J (2003) Reactive oxygen species and hormonal control of cell death. *Trends Plant Sci* **8**: 335–342
- Pell EJ, Schlaghauser CD, Arteca RN (1997) Ozone-induced oxidative stress: mechanisms of action and reaction. *Physiol Plant* **100**: 264–273
- Percy KE, Manninen S, Häberle KH, Heerd C, Werner H, Henderson GW, Matyssek R (2009) Effect of 3 years' free-air exposure to elevated ozone on mature Norway spruce (*Picea abies* (L.) Karst.) needle epicuticular wax physicochemical characteristics. *Environ Pollut* **157**: 1657–1665
- Porra RJ, Thompson WA, Kriedemann PE (1989) Determination of accurate extinction coefficients and simultaneous equations for assaying chlorophyll-a and chlorophyll-b extracted with 4 different solvents: verification of the concentration of chlorophyll standards by atomic-absorption spectroscopy. *Biochim Biophys Acta* **975**: 384–394
- Preuss SB, Meister R, Xu Q, Urwin CP, Tripodi FA, Screen SE, Anil VS, Zhu S, Morrell JA, Liu G, et al (2012) Expression of the *Arabidopsis thaliana* BBX32 gene in soybean increases grain yield. *PLoS ONE* **7**: e30717
- Raffaele S, Vaillau F, Léger A, Joubès J, Miersch O, Huard C, Blée E, Mongrand S, Domergue F, Roby D (2008) A MYB transcription factor regulates very-long-chain fatty acid biosynthesis for activation of the hypersensitive cell death response in *Arabidopsis*. *Plant Cell* **20**: 752–767
- Ruijter JM, Ramakers C, Hoogaars WMH, Karlen Y, Bakker O, van den Hoff MJB, Moorman AFM (2009) Amplification efficiency: linking baseline and bias in the analysis of quantitative PCR data. *Nucleic Acids Res* **37**: e45
- Samuels L, Kunst L, Jetter R (2008) Sealing plant surfaces: cuticular wax formation by epidermal cells. *Annu Rev Plant Biol* **59**: 683–707
- Sarkar A, Rakwal R, Bhushan Agrawal S, Shibato J, Ogawa Y, Yoshida Y, Kumar Agrawal G, Agrawal M (2010) Investigating the impact of elevated levels of ozone on tropical wheat using integrated phenotypic, physiological, biochemical, and proteomics approaches. *J Proteome Res* **9**: 4565–4584
- Skarby L, Troeng E, Bostrom CA (1987) Ozone uptake and effects on transpiration, net photosynthesis, and dark respiration in Scots pine. *For Sci* **33**: 801–808
- Stevenson DS, Dentener FJ, Schultz MG, Ellingsen K, van Noije TPC, Wild O, Zeng G, Amann M, Atherton CS, Bell N, et al (2006) Multi-model ensemble simulations of present-day and near-future tropospheric ozone. *J Geophys Res Atmos* **111**: D08301
- Stitt M, Sulpice R, Keurentjes J (2010) Metabolic networks: how to identify key components in the regulation of metabolism and growth. *Plant Physiol* **152**: 428–444

- Streeter JG, Lohnes DG, Fioritto RJ** (2001) Patterns of pinitol accumulation in soybean plants and relationships to drought tolerance. *Plant Cell Environ* **24**: 429–438
- Unsworth MH, Lesser VM, Heagle AS** (1984) Radiation interception and the growth of soybeans exposed to ozone in open-top field chambers. *J Appl Ecol* **21**: 1059–1079
- Vahisalu T, Puzõrjova I, Brosché M, Valk E, Lepiku M, Moldau H, Pechter P, Wang Y-S, Lindgren O, Salojärvi J, et al** (2010) Ozone-triggered rapid stomatal response involves the production of reactive oxygen species, and is controlled by SLAC1 and OST1. *Plant J* **62**: 442–453
- Vingarzan R** (2004) A review of surface ozone background levels and trends. *Atmos Environ* **38**: 3431–3442
- Von Caemmerer S, Farquhar GD** (1981) Some relationships between the biochemistry of photosynthesis and the gas exchange of leaves. *Planta* **153**: 376–387
- Welles JM, Norman JM** (1991) Instrument for indirect measurement of canopy architecture. *Agron J* **83**: 818–825
- Wilkinson S, Mills G, Illidge R, Davies WJ** (2012) How is ozone pollution reducing our food supply? *J Exp Bot* **63**: 527–536
- Zhang LX, Kyei-Boahen S, Zhang J, Zhang MH, Freeland TB, Watson CE, Lui X** (September 27, 2007) Modifications of optimum adaptation zones for soybean maturity groups in the USA. *Crop Management* <http://dx.doi.org/10.1094/CM-2007-0927-01-RS>
- Zhu X-G, Long SP, Ort DR** (2010) Improving photosynthetic efficiency for greater yield. *Annu Rev Plant Biol* **61**: 235–261